(NASA-CR-199800) PREDICTION OF MICROCRACKING IN COMPOSITE LAMINATES UNDER THERMOMECHANICAL LOADING (MIT) 8 p

N96-15862

Unclas

G3/24 0083960

PREDICTION OF MICROCRACKING IN COMPOSITE LAMINATES UNDER THERMOMECHANICAL LOADING

Jason R. Maddocks and Hugh L. McManus
Department of Aeronautics and Astronautics, Massachusetts Institute of Technology,
Cambridge, MA 02139, USA

ABSTRACT

Composite laminates used in space structures are exposed to both thermal and mechanical loads. Cracks in the matrix form, changing the laminate thermoelastic properties. An analytical methodology is developed to predict microcrack density in a general laminate exposed to an arbitrary thermomechanical load history. The analysis uses a shear lag stress solution in conjunction with an energy-based cracking criterion. Experimental investigation was used to verify the analysis. Correlation between analysis and experiment is generally excellent. The analysis does not capture machining-induced cracking, or observed delayed crack initiation in a few ply groups, but these errors do not prevent the model from being a useful preliminary design tool.

BACKGROUND

The attractive properties of advanced composite materials make them ideal candidates for space structures. However, mechanical loads and wide swings in temperature cause cracks in the matrix, called microcracks. They can have a profound effect on the thermoelastic properties of the laminate, with potentially disastrous consequences in dimensionally critical applications.

Prediction of microcracking under mechanical loading has been studied extensively. Many analyses have used *in situ* transverse ply strength as the cracking criterion. Lee & Daniel [1], for example, combined this failure criterion with a modified shear lag stress solution. Allen *et al.* [2] calculated damage with the internal state variable concept. Peters *et al.* [3] used a shear lag stress solution and Weibull strength distributions. However, Flaggs & Kural [4] questioned the validity of the strength-based approaches in general cases, showing that *in situ* ply strength is laminate dependent. Others have used fracture mechanics based cracking criteria. Laws & Dvorak [5] proposed a progressive damage model which incorporates a shear lag stress solution. Nairn *et al.* [6] and Varna & Berglund [7] used variational solutions of the stress fields. Wang & Crossman [8] and Binienda *et al.* [9] calculated stress distributions with finite element models. Nuismer & Tan [10] combined a two-dimensional elasticity model with a fracture mechanics cracking criterion.

Although many of the mechanical loading analyses have incorporated a residual thermal stress, very few predictive methodologies exist for progressive thermal loading. Most thermal analyses have focused only on the effects of microcracking on laminate properties. Bowles [11] and Adams & Herakovich [12], for instance, used finite element models to determine how coefficient of thermal expansion (CTE) is affected. Tompkins *et al.* [13] and Camahort *et al.* [14] experimentally determined the effects of thermal cycling on laminate thermoelastic properties. Some studies have been done to predict the onset of cracking (e.g. [15]). McManus *et al.* [16] developed an analytical method for thermally loaded cross-ply laminates. Crack density and reduced laminate properties were predicted as functions of monotonically decreasing temperature. The effects of thermal cycling were included in the analysis using a material degradation fatigue model. Experimentally, specimens were monotonically cooled or thermally cycled. Cracks were

subsequently counted on the edges. The analyses correlated very well with experiments. The work was later extended by Park [17] to predict crack density in all plies of general angle laminates. Analytical predictions agreed well with average interior crack densities measured experimentally. Park showed that, due to edge effects, interior crack counts are a better indicator of the laminate damage state than edge counts for other than cross-ply laminates.

STATEMENT OF PROBLEM

The objective of the present work is to develop an analytical methodology to predict the initiation and extent of microcracking in composite laminates under both thermal and mechanical loading. Analytical modeling in conjunction with experimental investigation is used to achieve this objective. An analysis is developed which, given material properties, laminate geometry, and load history, predicts crack densities and degraded laminate properties. Experimental work (i) provides verification of the analysis and (ii) allows a greater qualitative understanding of the problem. Finally, correlations provide insight into the details of the mechanisms by which microcracks form.

ANALYTICAL METHODS

Fig. 1 shows a laminate aligned with a global coordinate system xyz. The laminate is made up of unidirectional plies. Stacked plies with the same ply angle are assumed to act as a single thick ply, referred to as a ply group or layer. Cracks are assumed to span the layer thickness and propagate parallel to the fibers through the width of the laminate. Fig. 1 shows cracks of this type in a laminate with three ply groups. A local coordinate system $x'y'z'$ is defined for each crack. The y' axis is aligned with the crack, parallel to the fiber direction of the layer, the x' axis is aligned with the transverse direction of the layer, and the origin is at the center of the crack.

To predict cracking in any one ply group, the laminate is modeled as being made up of two components: the cracking layer and the smeared properties of the rest of the laminate, henceforth represented by the subscripts c and r, respectively. A one-dimensional shear lag model, as shown in Fig. 2, is used to determine the stress and displacement distributions in the vicinity of a crack in its local $x'y'z'$ coordinate system. In the shear lag solution that follows, E, α, u, and σ are the stiffness, CTE, displacement, and normal stress, respectively, in the x' direction. E_o is the effective laminate stiffness in the x' direction. The shear stress between uncracked and cracked layers in the $x'y'$ plane is q. The thicknesses of the cracking layer and the rest of the laminate are a_c and a_r, respectively, and a_o is the total laminate thickness. The laminate is subjected to a thermal load ΔT, which is the difference between the current temperature and some stress-free temperature, and an applied stress σ_a, where

$$\sigma_a = \frac{N_{x'}}{a_0} \tag{1}$$

$N_{x'}$ is the laminate load in the x' direction. From laminate equilibrium,

$$\sigma_a a_0 = \sigma_r a_r + \sigma_c a_c \tag{2}$$

From equilibrium of the cracked layer and the rest of the laminate,

$$q = \frac{a_c}{2}\frac{d\sigma_c}{dx'} \qquad q = -\frac{a_r}{2}\frac{d\sigma_r}{dx'} \tag{3}$$

The stress-strain relations for the layers are

$$\frac{\sigma_c}{E_c} = \frac{du_c}{dx'} - \alpha_c \Delta T \qquad \frac{\sigma_r}{E_r} = \frac{du_r}{dx'} - \alpha_r \Delta T \tag{4}$$

Substituting $q = K(u_c - u_r)$ (where K is an effective shear stiffness) into Eqns (3) and taking the derivative in x',

$$K\left(\frac{du_c}{dx'} - \frac{du_r}{dx'}\right) = \frac{a_c}{2}\frac{d^2\sigma_c}{dx'^2} \qquad K\left(\frac{du_c}{dx'} - \frac{du_r}{dx'}\right) = -\frac{a_r}{2}\frac{d^2\sigma_r}{dx'^2} \tag{5}$$

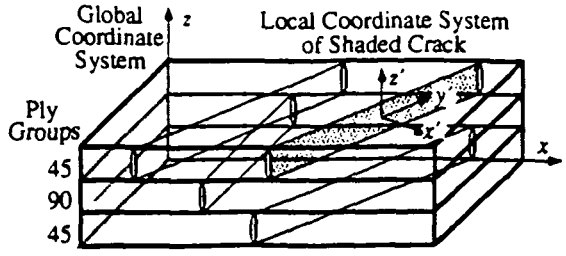

Figure 1. Laminate geometry

Combining Eqns. (4), multiplying by K, and substituting into Eqn. (5a),

$$\frac{d^2\sigma_c}{dx'^2} = \frac{2K}{a_c}\left[\frac{\sigma_c}{E_c} - \frac{\sigma_r}{E_r} + (\alpha_c - \alpha_r)\Delta T\right] \tag{6}$$

Solving Eqn. (2) for σ_r, substituting into Eqn. (6), and rearranging,

$$\frac{d^2\sigma_c}{dx'^2} - 2K\left(\frac{a_rE_r + a_cE_c}{a_ra_cE_rE_c}\right)\sigma_c = \frac{2K}{a_c}\left[-\frac{\sigma_a a_0}{a_rE_r} + (\alpha_c - \alpha_r)\Delta T\right] \tag{7}$$

Let

$$\zeta = \sqrt{\frac{Ka_c(a_rE_r + a_cE_c)}{2a_rE_rE_c}} \tag{8}$$

$$\lambda = \frac{2K(a_rE_r + a_cE_c)\sigma_a}{a_ra_cE_rE_0} - \frac{2K}{a_c}(\alpha_c - \alpha_r)\Delta T \tag{9}$$

where ζ is the shear lag parameter, a dimensionless quantity that includes both material properties and geometry, and λ is used for convenience. From the rule of mixtures,

$$a_0E_0 = a_rE_r + a_cE_c \tag{10}$$

Substituting Eqns. (8), (9), and (10) into Eqn. (7) gives

$$\frac{d^2\sigma_c}{dx'^2} - \frac{4\zeta^2}{a_c^2}\sigma_c = -\lambda \tag{11}$$

This has a solution of the form,

$$\sigma_c = A\sinh\left(\frac{2\zeta x'}{a_c}\right) + B\cosh\left(\frac{2\zeta x'}{a_c}\right) + \frac{\lambda a_c^2}{4\zeta^2} \tag{12}$$

Applying boundary conditions $\sigma_c = 0$ at $x' = \pm h$ gives

$$A = 0 \qquad B = \frac{-\lambda a_c^2}{4\zeta^2\cosh(2\zeta h/a_c)} \tag{13}$$

Placing Eqns. (13) into Eqn. (12), substituting Eqn. (9) into the result, and rearranging,

$$\sigma_c = \frac{Ka_c}{2\zeta^2}\left[\frac{(a_rE_r + a_cE_c)\sigma_a}{a_rE_rE_0} - (\alpha_c - \alpha_r)\Delta T\right]\left[1 - \frac{\cosh(2\zeta x'/a_c)}{\cosh(2\zeta h/a_c)}\right] \tag{14}$$

Solving Eqn. (2) for σ_r, substituting into Eqn. (14), and rearranging gives

$$\sigma_r = \frac{\sigma_a a_0}{a_r} - \frac{Ka_c^2}{2\zeta^2 a_r}\left[\frac{(a_rE_r + a_cE_c)\sigma_a}{a_rE_rE_0} - (\alpha_c - \alpha_r)\Delta T\right]\left[1 - \frac{\cosh(2\zeta x'/a_c)}{\cosh(2\zeta h/a_c)}\right] \tag{15}$$

Substituting Eqn. (14) into Eqn. (4a), solving for du_c and integrating from 0 to x',

$$u_c = \frac{Ka_c x'}{2\zeta^2 E_c}\left[\frac{(a_r E_r + a_c E_c)\sigma_a}{a_r E_r E_0} + \alpha_r \Delta T\right]\left[1 - \frac{a_c}{2\zeta x'}\frac{\sinh(2\zeta x'/a_c)}{\cosh(2\zeta h/a_c)}\right] + \frac{\alpha_c \Delta T x'}{2\zeta^2 E_c}\left[2\zeta^2 E_c - Ka_c\left(1 - \frac{a_c}{2\zeta x'}\frac{\sinh(2\zeta x'/a_c)}{\cosh(2\zeta h/a_c)}\right)\right] \tag{16}$$

Substituting Eqn. (15) into Eqn. (4b), solving for du_r and integrating from 0 to x,'

$$u_r = \frac{\sigma_a K a_c^2 x'}{2\zeta^2 a_r E_r}\left[\frac{2a_0\zeta^2}{Ka_c^2} - \frac{(a_r E_r + a_c E_c)}{a_r E_r E_0}\left(1 - \frac{a_c}{2\zeta x'}\frac{\sinh(2\zeta x'/a_c)}{\cosh(2\zeta h/a_c)}\right)\right] + \frac{\Delta T K a_c^2 x'}{2\zeta^2 a_r E_r}\left[\frac{2\zeta^2 a_r E_r \alpha_r}{Ka_c^2} + (\alpha_c - \alpha_r)\left(1 - \frac{a_c}{2\zeta x'}\frac{\sinh(2\zeta x'/a_c)}{\cosh(2\zeta h/a_c)}\right)\right] \tag{17}$$

The constants of integration in Eqns. (16) and (17) drop out because $u_r(0) = u_c(0) = 0$.

A new crack forms when the energy released due to crack formation, the strain energy release rate ΔG, is greater than the energy required to form a new surface, the critical strain energy release rate G_{Ic}. Assuming an existing uniform crack spacing $2h$, a new crack will instantaneously appear midway between two existing cracks when this failure criterion is met, as shown in Fig. 3. The minimum crack density at this load increment is defined as ρ, where $\rho = 1/(2h)$.

G_{Ic} is assumed to be a material property. ΔG is calculated from a Griffith energy balance,

$$\Delta G = \frac{\Delta W - \Delta U}{a_c} \tag{18}$$

where ΔW and ΔU are the changes in external work and internal strain energy, respectively, between the states before and after the hypothetical new crack forms. The strain energy contributions from normal stresses, U_σ, and shear stresses, U_q, are

$$U_\sigma = \frac{1}{2}\oint_v \frac{\sigma^2}{E}dV \qquad U_q = \frac{1}{2}\oint_v \frac{q^2}{G}dV \tag{19}$$

The total strain energy is $U = U_\sigma + U_q$. The change in strain energy when a new crack appears is found by subtracting the strain energy of the representative volume before the crack forms, where the cracks are separated by $2h$, from that after formation, where the cracks are h apart:

$$\Delta U = \left[2U|_h - U|_{2h}\right] \tag{20}$$

Solving Eqn. (20) yields

$$\Delta U = \frac{a_0^2 a_c^2 E_c \sigma_a^2 - a_r^2 a_c^2 E_r^2 E_c (\alpha_c - \alpha_r)^2 \Delta T^2}{2\zeta a_r a_0 E_r E_0}\left[2\tanh\left(\frac{\zeta h}{a_c}\right) - \tanh\left(\frac{2\zeta h}{a_c}\right)\right] \tag{21}$$

Note that there is no coupling between the thermal and mechanical loading in Eqn. (21). However,

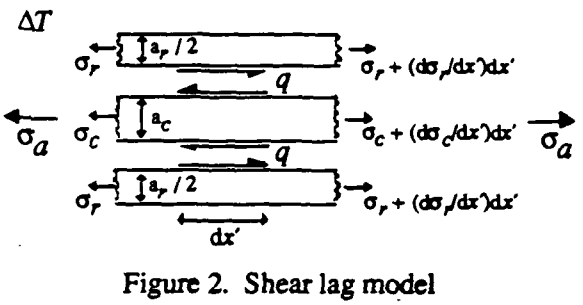

Figure 2. Shear lag model

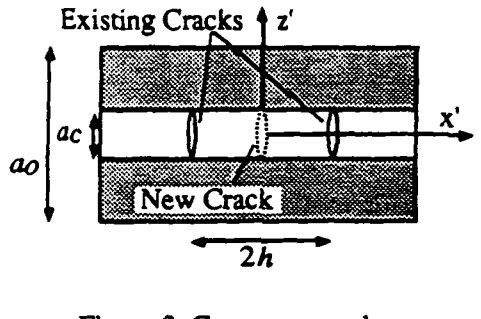

Figure 3. Geometry used in energy calculations

the work done by the applied loading is

$$W = \sigma_a a_0 u_r \tag{22}$$

The change in external work when a crack forms is given by

$$\Delta W = \left[2W|_h - W|_{2h}\right] \tag{23}$$

Placing Eqn. (17) into Eqn. (22) and solving Eqn. (23),

$$\Delta W = \frac{2a_0^2 a_c^2 E_c \sigma_a^2 - 2a_0 a_r a_c^2 E_r E_c (\alpha_c - \alpha_r)\sigma_a \Delta T}{2\zeta a_0 a_r E_r E_0}\left[2\tanh\left(\frac{\zeta h}{a_c}\right) - \tanh\left(\frac{2\zeta h}{a_c}\right)\right] \tag{24}$$

Placing Eqns. (21) and (24) into Eqn. (18) gives the total change in strain energy release rate:

$$\Delta G = \frac{a_c E_c}{2\zeta a_0 a_r E_r E_0}\left[a_0\sigma_a - a_r E_r(\alpha_c - \alpha_r)\Delta T\right]^2\left[2\tanh\left(\frac{\zeta h}{a_c}\right) - \tanh\left(\frac{2\zeta h}{a_c}\right)\right] \tag{25}$$

It is important to note that the final expression for ΔG has a thermomechanical interaction term due to the coupling between thermal and mechanical loading in Eqn. (24). Note also that Eqn. (25) must be solved numerically or graphically to find h (or ρ) for a given ΔT and σ_a.

At every load increment, the crack formation analysis is carried out for each ply group in turn. The properties of the ply group considered are calculated in its local coordinate system $x'y'z'$ using familiar CLPT relations, and knockdown factors to account for existing cracks. Next, Eqn. (25) is used to determine the new crack density in that layer. Once all of the ply groups have been examined at this load increment, the effective laminate properties are updated. The cycle is repeated for each load increment until the entire load history is completed. This iterative damage progression model is implemented by the computer code CRACKOMATIC II, available by request from the authors, which takes material properties, laminate geometry, and thermomechanical load history and outputs crack density and degraded laminate properties. The analysis and its implementation are presented in detail in [18].

EXPERIMENTAL PROCEDURES

Experiments were conducted to correlate with analytical predictions and to investigate the microcracking problem qualitatively. AS4/3501-6 graphite epoxy laminates were fabricated at the Technology Laboratory for Advanced Composite Materials at MIT using 0.127 mm (0.005") thick plies. Three different layups, $[0_4/45_4/90_4/-45_4]_S$, $[0_2/45_2/90_2/-45_2]_S$, and $[0_2/60_2/-60_2]_S$, were manufactured to investigate laminate geometry and thickness effects. Panels were cut into test specimens according to the matrix in Table 1. Both long edges of every specimen were polished to minimize crack initiation sites and to facilitate microscopic inspection. All specimens were dried and then stored in desiccant to eliminate moisture.

Thermal specimens were monotonically cooled to progressively lower temperatures in an environmental chamber. Starting at room temperature, the specimens were cooled to temperatures as low as -184°C (-300°F) at a rate of 14°C/min. The cooling and heating rates were low enough to avoid significant thermal gradients. Specimens were soaked at the target temperature for 5 minutes and returned to room temperature. The edges of the specimens were then inspected for cracks under an optical microscope at 100× magnification. Sacrificial thermal specimens were sanded to

Table 1. Test matrix repeated for all 3 layups

Testing/Data	Dimensions (cm)	Total Specimens
Thermal/Edge	7.62 x 2.54	5
	7.62 x 1.27	5
Thermal/Interior	7.62 x 2.54	15
	7.62 x 1.27	15
Mechanical/Edge	25.4 x 2.54	5

Table 2. Material properties

E_l (GPa)	142.0	α_l (με/°C)	-0.36
E_t (GPa)	9.81	α_t (με/°C)	28.8
ν	0.30	G_{Ic} (J.m^2)	141.0
G_{lt} (GPa)	6.0	ζ	1.0

incremental depths to measure interior crack densities. An observed crack extending more than half the thickness of a ply or ply group was counted as a crack. Mechanical coupons were loaded under monotonically increasing tension at room temperature. Edge crack data was collected at incremental loads until failure or other damage modes, such as delamination, were observed.

RESULTS

Material data used in the analyses are presented in Table 2. The same values of the shear lag parameter, ζ, and the critical strain energy release rate, G_{Ic}, were used for all analyses. In each of the following figures, the measured and predicted crack densities for specified ply groups are shown as functions of the mechanical or thermal load. The results for the 45_4 and 90_4 ply groups in mechanically loaded $[0_4/45_4/90_4/-45_4]_S$ laminates are shown in Fig. 4. The 45_4 ply group begins cracking at a higher load and accumulates less cracks than the 90_4 layer. The scatter is relatively low, except in the region where cracking initiates. The analysis successfully predicts the onset of cracking and only slightly underpredicts the accumulation of cracks in both layers. The same trends are seen in the 45_2 and 90_2 ply groups in the $[0_2/45_2/90_2/-45_2]_S$ laminates, shown in Fig. 5. Note that cracking initiates at nearly identical loads in both laminates, even though the latter are half as thick. Additionally, the thinner $[0_2/45_2/90_2/-45_2]_S$ laminates reach significantly higher crack densities than the $[0_4/45_4/90_4/-45_4]_S$ laminates.

The analysis does not predict the initiation of cracking in the middle ply groups under mechanical loading satisfactorily. Cracking initiates in these layers only when the adjacent layers start to crack, even though the analysis predicts cracking much earlier. However, the analysis appears to capture microcrack accumulation once cracking has begun, as shown by the $[0_2/60_2/-60_2]_S$ results in Fig. 6. Here cracking is suppressed in the -60_4 layer until the load reaches 13kN, when cracking initiates in the adjacent 60_2 layers. Once the -60_4 layer begins to crack, the analysis predicts crack density in that layer nearly perfectly. Correlation between analysis and experiment in the 60_2 layer is very good throughout the entire range of microcracking.

Thermal loading data and analyses for the 45_4 and 90_4 ply groups in the $[0_4/45_4/90_4/-45_4]_S$ laminates are shown in Fig. 7. Scatter in the thermal data is generally higher than in the mechanical data. The analysis captures the cracking behavior of the 45_4 layer, including initiation temperature and crack accumulation. Some initial cracks were present in the 90_4 ply group after manufacture, which the analysis does not predict. Nevertheless, the analysis appears to successfully predict crack density in this layer at the lowest temperature increments.

The thermal data does not manifest the middle ply problem described earlier for the mechanical data. Cracking initiation in the middle layers is not influenced by adjacent layers. For example, the analysis predicts initiation and accumulation in the -45_8 ply groups in the $[0_4/45_4/90_4/-45_4]_S$ laminates very well, shown in Fig. 8. Fig. 9 shows the thermal loading data and analyses for the 45_2 and 90_2 ply groups in the $[0_2/45_2/90_2/-45_2]_S$ laminates. Little cracking was observed in these laminates under thermal loading. The analysis predicts no cracking down to -184°C, agreeing well with experiment, as virtually no cracks were observed in the 45_2 layer. The onset of cracking in the 90_2 layer is later than predicted, but the analysis agrees well with the data at the lowest temperature. Unfortunately, it is difficult to assess the correlation between experiment and analysis for this layup, as so few data points are available. The $[0_2/60_2/-60_2]_S$ laminates do not crack at all under thermal loading, even though the analysis predicts initiation in all layers.

DISCUSSION AND CONCLUSIONS

1. The present methodology shows promise as a powerful, unified analytical tool for predicting microcracking in all plies of a general angle laminate exposed to an arbitrary thermomechanical load history. It could be useful in any application of composites where dimensional stability is critical and the structure is exposed to a combination of thermal and mechanical loads.

2. Its general applicability is further bolstered by the fact that the shear lag and fracture mechanics parameters do not demonstrate laminate dependence to an acceptable approximation. Thus they only need to be measured once for a given material system. This can be done by counting cracks in a cross-ply laminate under tension and using the analysis to back out the parameters.

3. The limits of the analysis need further exploration. Different material systems, or very thick or very thin ply groups, may have different mechanisms of damage that fall outside of the assumptions used in the model presented here.

4. The analysis assumes that critical starter cracks are inherent in the uncracked laminate. If these flaws are edge defects, then laminates with a strong edge effect (see [18]) may experience delayed onset of cracking. Cracking in a layer is then initiated instead by stress concentrations from cracks in adjacent layers. This offers an explanation for the delayed onset of cracking in some layers under mechanical loading. This could also explain why the $[0_2/60_2/-60_2]_S$ laminates, which have a strong edge effect, did not crack under thermal loading.

5. Even though the analysis does not capture crack initiation in some layers under mechanical loading, it predicts crack accumulation very well after the onset of cracking. The analysis also sometimes predicts cracking when none are observed experimentally, such as the thermal loading of the $[0_2/60_2/-60_2]_S$ laminates. The methodology is conservative in these cases, and works well in all others considered. Hence it appears to be a very useful analytical tool.

Acknowledgment: This work was supported by NASA Grant NAG-1-1463, supervised by Steve Tompkins.

REFERENCES

1. J. Lee and I. Daniel, Progressive Transverse Cracking of Crossply Composite Laminates. *J. Comp. Mater.* **24**, 1225-1243 (1990).
2. D. Allen and J. Lee, Matrix Cracking in Laminated Composites under Monotonic and Cyclic Loadings. *Microcracking-Induced Damage in Comp.*, ASTM, Dallas, 65-75 (1990).
3. P. Peters and T.-W. Chou, On cross-ply cracking in glass and carbon fibre-reinforced epoxy laminates. *Composites* **18** (1), 40-46 (1987).
4. D. Flaggs and M. Kural, Experimental Determination of the In Situ Transverse Lamina Strength in Graphite/Epoxy Laminates. *J. Comp. Mater.* **16**, 103-116 (1982).
5. N. Laws and G. Dvorak, Progressive Transverse Cracking in Composite Laminates. *J. Comp. Mater.* **22**, 900-916 (1988).
6. S. Liu and J. Nairn, The Formation and Propagation of Matrix Microcracks in Cross-Ply Laminates during Static Loading. *J. Reinf. Plast. and Comp.* **11**, 158-178 (1992).
7. J. Varna and L. Berglund, Multiple Transverse Cracking and Stiffness Reduction in Cross-Ply Laminates. *J. Comp. Techn. and Res.* **13** (2), 99-106 (1991).
8. F. Crossman and A. Wang, The Dependence of Transverse Cracking and Delamination on Ply Thickness in Graphite/Epoxy Laminates. *Damage in Composite Materials, ASTM STP 775*, 118-139 (1982).
9. A. Gyekenyesi, J. Hemann, and W. Binienda, Crack Development in Carbon/Polyimide Cross-Ply Laminates under Uniaxial Tension. *SAMPE J.* **30** (3), 17-28 (1994).
10. S. Tan and R. Nuismer, A Theory for Progressive Matrix Cracking in Composite Laminates. *J. Comp. Mater.* **23**, 1029-1047 (1989).
11. D. Bowles, Effect of Microcracks on the Thermal Expansion of Composite Laminates. *J. Comp. Mater.* **18**, 173-187 (1984).
12. D. Adams and C. Herakovich, Influence of Damage on the Thermal Response of Graphite-Epoxy Laminates. *J. Thermal Stresses* 7, 91-103 (1984).
13. S. Tompkins, Effects of Thermal Cycling on Composite Materials for Space Structures. *NASA/SDIO Space Environmental Effects on Mater. Workshop*, 447-470 (1989).
14. J. Camahort, E. Rennhack, and W. Coons, Effects of Thermal Cycling Environment on Graphite/Epoxy Composites. *Environmental Effects on Adv. Comp. Mater., ASTM STP 602*, 37-49 (1976).
15. D. Bowles, S. Tompkins, and J. Funk, Residual Thermal Stresses in Composites for Dimensionally Stable Spacecraft Applications. *SEM Seventh Int. Congress on Exper. Mech.*, Las Vegas, NV (1992).
16. H. McManus, D. Bowles, and S. Tompkins, Prediction of Thermally Induced Matrix Cracking. *Proc. of the American Soc. of Comp.*, Cleveland, Ohio (1993).
17. C. Park and H. McManus, Thermally Induced Damage in Composite Space Structure: Predictive Methodology and Experimental Correlation. *Comp. Sci. and Tech.* (1995).
18. J. Maddocks, Microcracking in Composite Laminates Under Thermal and Mechanical Loading. Massachusetts Institute of Technology, Masters Thesis (1995).

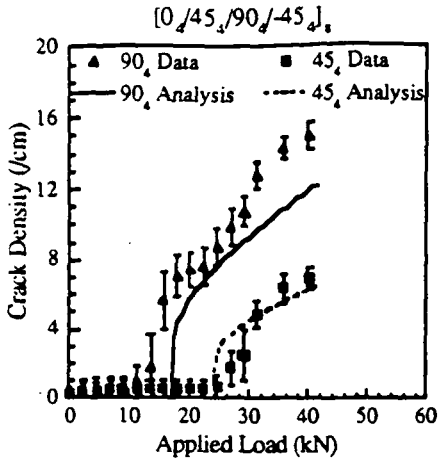

Figure 4. Mechanical loading of 32-ply specimens

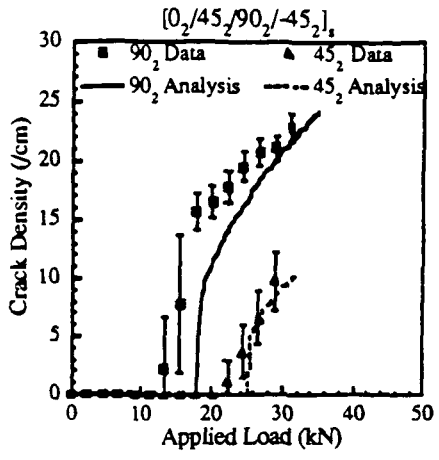

Figure 5. Mechanical loading of 16-ply specimens

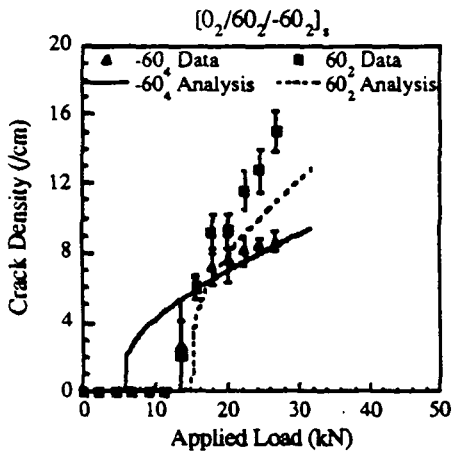

Figure 6. Delayed initiation of cracking in middle layer under mechanical loading

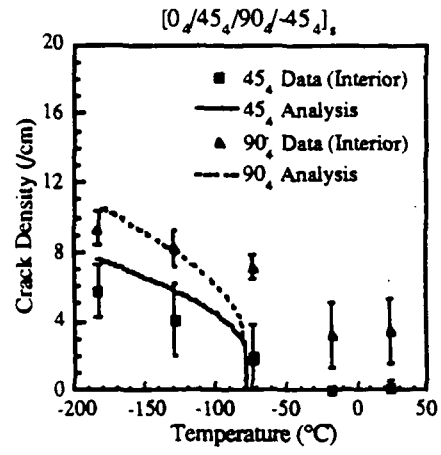

Figure 7. Thermal loading data in 32-ply specimens

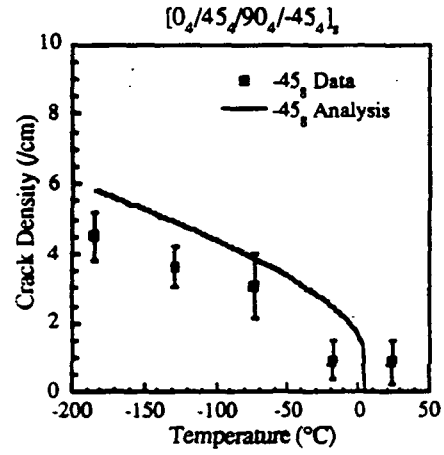

Figure 8. Thermal data; 32-ply specimens

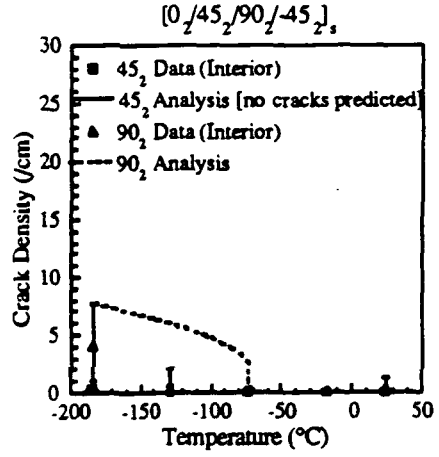

Figure 9. Thermal data; 16-ply specimens